doi:10.1093/brain/awr237 Brain 2011: 134; 3236–3248 | 3236

BRAIN
A JOURNAL OF NEUROLOGY

Reduced ventricular proliferation in the foetal cortex following maternal inflammation in the mouse

Helen B. Stolp,[1,2] Casmir Turnquist,[1] Katarzyna M. Dziegielewska,[2] Norman R. Saunders,[2] Daniel C. Anthony[3] and Zoltán Molnár[1]

1 Department of Physiology, Anatomy and Genetics, University of Oxford, Oxford OX1 3QX and St John's College Research Centre, Oxford OX1 3JP, UK
2 Department of Pharmacology, University of Melbourne, Parkville 3010, Australia
3 Department of Pharmacology, University of Oxford, Oxford QX1 3QT, UK

Correspondence to: Dr Helen Stolp,
Department of Physiology,
Anatomy and Genetics,
Le Gros Clark Building,
University of Oxford,
South Parks Road,
Oxford OX1 3QX, UK
E-mail: helen.stolp@dpag.ox.ac.uk

It has been well established that maternal inflammation during pregnancy alters neurological function in the offspring, but its impact on cortical development and long-term consequences on the cytoarchitecture is largely unstudied. Here we report that lipopolysaccharide-induced systemic maternal inflammation in C57Bl/6 mice at embryonic Day 13.5 of pregnancy, as early as 8 h after challenge, caused a significant reduction in cell proliferation in the ventricular zone of the developing cerebral cortex, as revealed by quantification of anti-phospho-Histone H3 immunoreactivity and bromodeoxyuridine pulse labelling. The angle of mitotic cleavage, determined from analysis of haematoxylin and eosin staining, cyclin E1 gene expression and the pattern of β-catenin immunoreactivity were also altered by the challenge, which suggests a change from symmetric to asymmetric division in the radial progenitor cells. Modifications of cortical lamination and gene expression patterns were detected at post-natal Day 8 suggesting prolonged consequences of these alterations during embryonic development. Cellular uptake of proteins from the cerebrospinal fluid was observed in brains from lipopolysaccharide-treated animals in radial progenitor cells. However, the foetal blood–brain barrier to plasma proteins remained intact. Together, these results indicate that maternal inflammation can disrupt the ventricular surface and lead to decreased cellular proliferation. Changes in cell density in Layers IV and V at post-natal Day 8 show that these initial changes have prolonged effects on cortical organization. The possible shift in the fate of progeny and the resulting alterations in the relative cell numbers in the cerebral cortex following a maternal inflammatory response shown here will require further investigation to determine the long-term consequences of inflammation on the development of neuronal circuitry and behaviour.

Keywords: proliferation; ventricular zone; inflammation; β-catenin; foetus

Abbreviations: pH3 = phospho-Histone H3; TUNEL = terminal deoxynucleotidyl transferase dUTP nick end labelling

Received March 15, 2011. Revised June 30, 2011. Accepted July 13, 2011. Advance Access publication September 29, 2011

Introduction

Maternal inflammation during pregnancy has been associated with neurodevelopmental disorders in children including autism, schizophrenia and cerebral palsy (Nelson and Grether, 1999; Pardo and Eberhart, 2007; O'Shea *et al.*, 2009; Brown, 2011). This has been supported by a large body of animal experiments that have revealed a link between maternal inflammation and altered behavioural outcomes in the offspring (Fatemi *et al.*, 2002, 2008*a*; Shi *et al.*, 2003; Meyer *et al.*, 2006; Nawa and Takei, 2006; Girard *et al.*, 2009; Stolp *et al*., 2011). However, the mechanism by which maternal inflammation can affect foetal brain development is uncertain.

Perinatal inflammation has been shown to produce a spectrum of long-term behavioural changes in rodents. The most commonly reported outcome is an impaired sensorimotor gaiting (prepulse inhibition; Shi *et al.*, 2003; Meyer *et al.*, 2005, 2006; Nyffeler *et al.*, 2006; Fortier *et al.*, 2007), while other behavioural changes include increased anxiety-like behaviour (Hava *et al.*, 2006), motor (Girard *et al.*, 2009) and cognitive deficits such as altered learning and memory (Golan *et al.*, 2005; Meyer *et al.*, 2005) and exploratory behaviour (Meyer *et al.*, 2005, 2006). Meyer *et al*. (2006) have shown that the nature of the behavioural alteration is dependent on when the challenge occurs within the normal developmental timetable.

In rodents, cortical neurogenesis occurs in the final week of the 3-week gestational period, which is approximately equivalent to middle of the first to middle of the second trimester (50–100 days) in humans (Rice and Barone, 2000; Clancy *et al.*, 2001, 2007). This period of development corresponds to a critical window for major human neurodevelopmental disorders (Rice and Barone, 2000; Rehn and Rees, 2005; Pardo and Eberhart, 2007). There are few studies examining the consequences of an inflammatory insult on cortical development, with the majority focused either at the beginning or end of neurogenesis and examining long-term outcomes (Fatemi *et al.*, 2002; Meyer *et al.*, 2006). Within the period of neurogenesis the correct proliferation, migration and subsequent differentiation of cells produced in the ventricular zone of the neocortex are essential for normal brain development and later cognitive function (Rakic and Caviness, 1995; Pramparo *et al.*, 2010; Wynshaw-Boris *et al.*, 2010).

Our study sought to examine the effect of maternal inflammation on proliferation in the developing neocortex as a potential contributor to long-term neurological and behavioural disorders. The results show for the first time that structural alterations in the foetal brain occur at the time of maternal inflammation and that structural changes persist into the post-natal period. These changes in forebrain development are likely to contribute to long-term neurological disorders in the offspring.

Materials and methods

Animal model and tissue preparation

Inflammation was induced by an intraperitoneal injection of 10 or 500 μg/kg lipopolysaccharide (*E. coli* 055:B5, Sigma-Aldrich) to female C57BL/6 mice at embryonic Day 13.5. Time-matched control animals were injected with an equal volume of saline (10 μl/g body weight). A subgroup of animals was injected intraperitoneally with 5-bromo-2-dioxyuridine (bromodeoxyuridine 100 mg/kg, Sigma) 2 h following lipopolysaccharide or saline injection. Animals were killed via cervical dislocation (dams) or decapitation (foetuses), 8 (embryonic Day 14) or 48 h (embryonic Day 15.5) after lipopolysaccharide or saline injection. Some animals were left until post-natal Day 8 and were perfusion fixed under terminal anaesthesia with saline followed by 4% paraformaldehyde (in 0.1 M phosphate buffer, pH 7.4). Animals kept to embryonic Day 15 or post-natal Day 8 received the 10 μg/kg dose of lipopolysaccharide. All animal procedures were conducted in accordance with institutional ethical guidelines and with UK Home Office approval (licence number 30/2524).

Tissue from foetal and post-natal Day 8 animals was fixed by immersion in 4% paraformaldehyde or Bouin's solution (Sigma-Aldrich). Paraformaldehyde-fixed tissue was embedded in 5% agar (Bioline, in phosphate-buffered saline) and 50-μm thick sections were cut using a vibrating blade microtome (VT1000S, Leica). Bouin's fixed sections were washed and dehydrated through increasing concentrations of ethanol and Histoclear (National diagnostics) before being embedded in paraffin. Coronal sections of 10 μm thickness were cut with a Reichert-Jung microtome. Fresh cortical tissue was collected from littermates for RNA extraction. Surface blood vessels were removed from the cortical hemispheres and tissue was stored in RNAlater® (Invitrogen) before RNA extraction using a TRIzol® protocol (Invitrogen).

Immunohistochemistry

To visualize bromodeoxyuridine, agar-embedded sections were treated with 1 M HCl at 40°C. They were washed in phosphate-buffered saline and Fc binding sites were blocked with 2% normal horse serum (in phosphate-buffered saline with 0.3% Triton X-100, Sigma) before incubation overnight in primary antibodies at 4°C. Proliferating cells were detected using mouse anti-bromodeoxyuridine primary antibodies (S Phase, 1 : 100, Progen) or rabbit anti-phospho-Histone H3 (pH3, M phase, 1 : 250, Abcam). Goat anti-mouse IgG-Alexa 488 or goat anti-rabbit IgG-Alexa 546 secondary antibodies (1 : 100, Abcam) were used to reveal the primary antibodies, respectively, and sections were counterstained with 4′,6-diamidino-2-phenylindole (DAPI) (1 : 1000 in phosphate-buffered saline). Control sections were stained without the addition of the primary antibody and showed no positive immunostaining (data not shown).

For paraffin immunohistochemistry, slides were heated to 65°C before being cleared and rehydrated. Sections were blocked in 1% H_2O_2 in phosphate-buffered saline–Tween-20 and then blocked in 5% normal horse serum in phosphate-buffered saline–Tween-20. Sections were incubated in primary antibodies in 1% horse serum in phosphate-buffered saline–Tween-20 overnight. Biotinylated secondary antibodies (goat anti-rabbit or goat anti-mouse, 1 : 100, Abcam) and horseradish peroxidase–streptavidin (Vector, 1 : 100) were used to reveal the immunoreaction. The reaction product was developed with diaminobenzidene. Primary rabbit antibodies against pH3 (as above), active caspase 3 (1:100, Abcam), and whole mouse serum (1 : 3000, Sigma-Aldrich) were used. Mouse antibodies to acetylated tubulin (1 : 200, Sigma) were used to detect radial progenitors, and antibodies against β-catenin (1 : 500; Abcam), claudin-5 and occludin (1 : 100, Zymed-Invitrogen) to assess junction structure were also employed. Pax6 (ventricular zone, 1 : 100, Covance) and Tbr2 (subventricular zone, 1 : 200, Abcam) antibodies were used to assess the proliferative zones at embryonic Day 15 and NeuN (pan-neuronal marker, 1 : 250, Chemicon), C_2H_2 zinc finger protein 2 (CTIP2) (Layer V,

1 : 400, Abcam) and RAR-related orphan receptor (ROR) (Layer IV, 1 : 200, R&D Systems) antibodies stained neuronal populations at post-natal Day 8.

Analysis of proliferating cells

Sections were photographed using a Leica DMR microscope and DFC 500 camera or imaged with Zeiss LSM710 confocal microscope. Cells were counted from images using UTHSCSA ImageTool. Paraffin sections from the level of the intraventricular foramina containing a sector of the putative primary somatosensory cortex were selected (equivalent to Bregma −0.4 in the adult brain). All proliferating cells in the cortex, both ventricular and subventricular zones, were counted for each hemisphere and the average number of cells per hemisphere was calculated from three to six sections per brain, two to three brains per litter and four litters per treatment. All analysis was performed blind. Confocal images across the entire depth of the cortex stained for bromodeoxyuridine were divided into five zones of 50 μm spanning from the ventricular to pial surface within a 200-μm wide sector. All positively stained cells were counted in each zone for each image taken with ×40 objective, from two sections per brain, two brains per litter and four litters per treatment.

Cells undergoing mitosis at the ventricular surface were also examined in haematoxylin and eosin-stained sections. All cells that were in anaphase in the dorsal cortex were photographed (from three sections per brain, Fig. 2H) and assessed for their angle of division in comparison with the ventricular surface using the UTHSCSA ImageTool (Fig. 2H). Data were separated into six groups based on the angle of mitosis (e.g. Group 1, 75–90°) and the proportion of cells was calculated for each brain (Cheung *et al*., 2010). Data were averaged from one to two animals per litter and a minimum of three litters were used per treatment.

Cell death

The presence of dying cells was examined using TUNEL (terminal deoxynucleotidyl transferase dUTP nick end labelling) staining in 50-μm thick vibratome sections. Sections were mounted on glass slides and air dried for 30 min, followed by dehydration and rehydration fixation in isopropanol. Sections were pre-treated with DNaseI buffer (Roche), and the positive control sections were treated with DNaseI (Roche) for 20 min at 37°C. Sections were incubated with the TUNEL reagent (Roche) at 37°C for 30 min before being counterstained with DAPI.

In parallel experiments, paraffin-embedded tissue sections were stained for the presence of the active caspase-3 protein using standard immunohistochemistry techniques as described above. Sections from at least two brains from three litters per treatment group were examined for cell death using a ×40 objective on a Leica DMR microscope.

Quantitative reverse transcription polymerase chain reaction

For the evaluation of Cyclin E1 expression, a cell cycle regulator, messenger RNA (500 ng per reaction) from foetal brains was converted to complementary DNA using SuperScript® III reverse transcriptase (Invitrogen) and thermal cycles of 5 min at 25°C, 60 min at 50°C, 25 min at 70°C. Quantitative reverse transcription polymerase chain reaction was conducted with a LightCycler® 480, using Roche Universal ProbeLibrary probes and LightCycler® mastermix (Roche). Primers are listed from 5′ to 3′; Cyclin E1 forward: TTCTGCAGC GTCATCCTCT; reverse: TGGAGCTTATAGACTTCGCACA; β-actin forward: CTAAGGCCAACCGTGAAAAG; reverse: ACCAGAGGCATA CAGGGACA. Samples were compared with an internal standard curve and β-actin expression for the same sample and are expressed as fold change compared with control brain values ($n = 7$ saline, $n = 4$ lipopolysaccharide, taken from three litters per treatment).

Proliferative zones at embryonic Day 15

Paraffin sections from the region of the intraventricular foramina were selected and were photographed using a Leica DMR microscope and DFC 500 camera. The area of immunoreactivity was assessed from images using UTHSCSA ImageTool. Lateral and medial columns (75 μm wide from ventricular to pial surfaces) were selected for measurements from each hemisphere and the average proportion of cortical stain per brain was calculated from two sections per brain, two to three brains per litter and three to four litters per treatment.

Cortical layering at post-natal Day 8

Sections from the region of the intraventricular foramina were selected and stained with neuronal subpopulation antibodies as described above. Each cerebral hemisphere was photographed and a 405-μm wide column was selected from S1, including the whole cortex from the white matter/grey matter boundary to the pial surface. The numbers of immunopositive cells were counted in the CTIP2- and ROR-stained sections using UTHSCSA ImageTool and the location of staining was compared with the whole cortical population from adjacent NeuN-stained sections. Two columns were counted from one to two brains per litter, three to four litters per treatment.

Data analysis

Data are presented as mean ± standard error of the mean (SEM). Unless otherwise stated, statistical comparisons are made between control (saline) and lipopolysaccharide- (10 μg/kg dose) treated animals using Student's *t*-test. Differences between means were considered statistically significant at $P \leqslant 0.05$.

Results

Proliferation and cell death

The results presented here are for animals treated with saline or 10 μg/kg lipopolysaccharide, unless otherwise stated. At embryonic Day 14 (embryonic Day 13.5 plus 8 h) the ventricular zone of the entire dorsal cortex of saline-treated animals had an average of 171 ± 18 pH3 immunopositive cells per section at the level of the intraventricular foramina, and in the subventricular zone there was an average of 31 ± 4 cells (Fig. 1). In the cortical ventricular zone of foetuses from treated dams, there was a significant decrease in the number of pH3-positive cells, which fell from 171 ± 18 to 92 ± 26 cells ($P = 0.047$, Fig. 1C and D). In the subventricular zone, a smaller number of mitotic cells (18 ± 5 in the dorsal cortex per section) was also detected, but this was not statistically significant compared with control numbers ($P = 0.1$). These results indicate that at 8 h following maternal-induced inflammation there is a reduction in mitosis in the foetal cortex (Fig. 1).

For embryonic Day 13.5 mice injected with lipopolysaccharide, followed by bromodeoxyuridine injection 2 h later and examined 8 h following lipopolysaccharide injection, an average of 92 ± 8 cells were labelled with bromodeoxyuridine per section in the dorsal

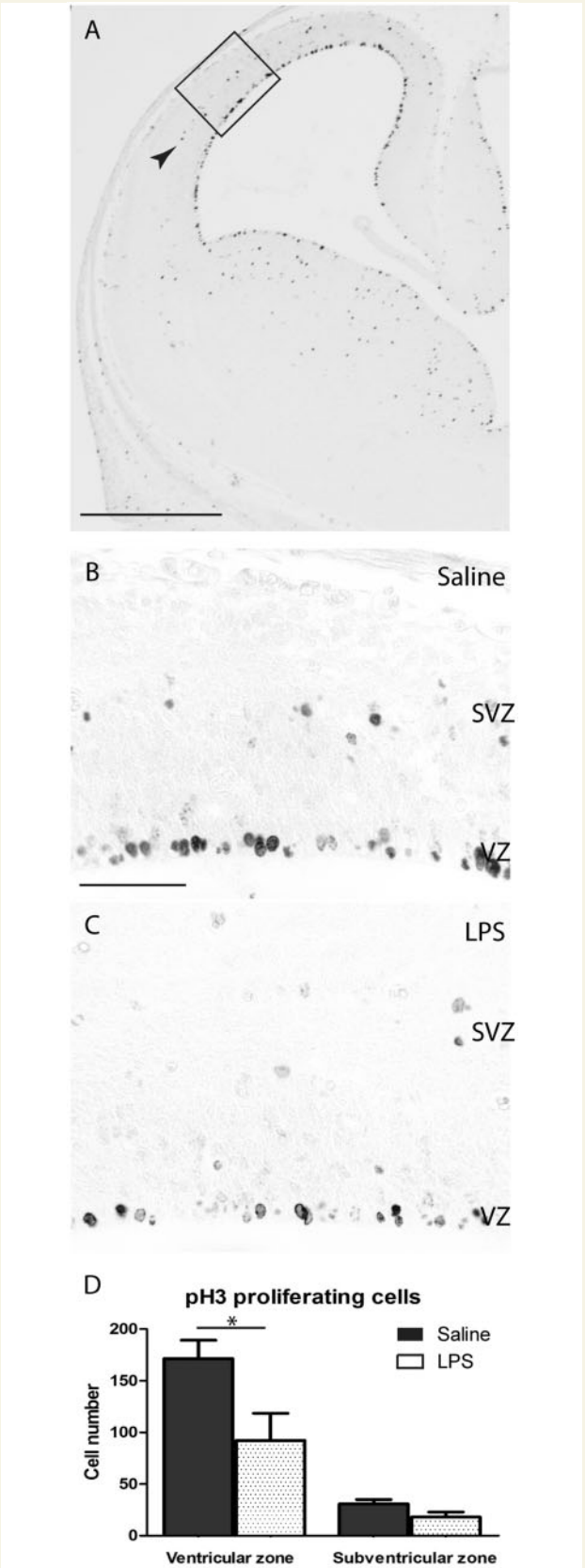

Figure 1 Comparison of the phospho-Histone H3 (pH3)-positive proliferating cells in the ventricular zone (VZ) and in the subventricular zone (SVZ, arrowhead in **A**) in saline- and lipopolysaccharide- (10 μg/kg) treated embryonic Day 13.5 animals at 8 h following injection (embryonic Day 14). In brains from lipopolysaccharide-treated dams fewer pH3 cells are observed (**C**) compared with saline-treated animals (**B**, higher magnification of boxed region in **A**). This difference was significantly different for the ventricular zone (**D**). Scale bar: **A** = 500 μm; **B**, **C** = 50 μm. *$P < 0.05$.

ventricular zone of control animals and there were fewer positively labelled cells in lipopolysaccharide-treated animals (65 ± 3, $P = 0.004$, Fig. 2). When the distance between the nucleus and the ventricular surface was determined, 60% of cells were found to lie within 50 μm of the ventricular surface in control animals, compared with 67% of cells from lipopolysaccharide-treated animals. This resulted in significantly fewer labelled nuclei in the deep portion of the ventricular zone in the lipopolysaccharide-treated animals, 21 ± 1 compared with 35 ± 4 in control animals ($P = 0.003$, Fig. 2A, D and G). Therefore, significantly fewer cells had entered the synthesis phase of cell division in the foetal cortex during the early phases of maternal inflammation. However, those cells undergoing synthesis appear to have faster interkinetic migration prior to mitosis. This is reflected in the percentage of cells that were pH3/bromodeoxyuridine positive (Fig. 2). In saline-treated animals, $87 \pm 8\%$ of the mitotic cells (pH3 positive) were also bromodeoxyuridine positive, and in the lipopolysaccharide-treated animals $95 \pm 3\%$ of the mitotic cells were double labelled (Fig. 2B, C, E and F). Most mitotic cells in both the saline- and lipopolysaccharide-treated animals went through mitosis with a cleavage plane near vertical (75–90°). However, the proportion of cells in this group was significantly reduced in lipopolysaccharide-treated animals ($62 \pm 5\%$ in controls, $47 \pm 7\%$ in lipopolysaccharide, $P = 0.05$, Fig. 2H), which reflected a general increase in cells with an angle of mitosis $<60°$. There was also a decrease in the expression of cyclin E1 in the cortex of foetuses from lipopolysaccharide-treated animals compared with controls, 6.5 ± 1.8 U (relative to β-actin) in saline-treated animals compared with 2.5 ± 0.9 U for lipopolysaccharide-treated animals, but this difference did not reach statistical significance ($P = 0.15$).

No TUNEL (Fig. 3A and B) or activated caspase-3-positive cells (Fig. 3C and D) were observed in the cortex of saline or either 10 μg or 500 μg/kg lipopolysaccharide-treated foetuses 8 h following treatment, indicating that the decrease in pH3-positive cells was not due to cell death following induction of inflammation in the dam.

Plasma protein uptake

The majority of proteins in the CSF (e.g. albumin) are plasma proteins found in the blood that are transferred into the CSF across the blood–CSF barrier by a specific and developmentally regulated transport mechanism (Dziegielewska *et al*., 1980; Habgood *et al*., 1992; Liddelow *et al*., 2009, 2011). Apart from fetuin in the early cortical plate (Dziegielewska *et al*., 1993) and several plasma proteins in the ventricular zone (Dziegielewska *et al*., 2000) of the developing brain that are transferred across

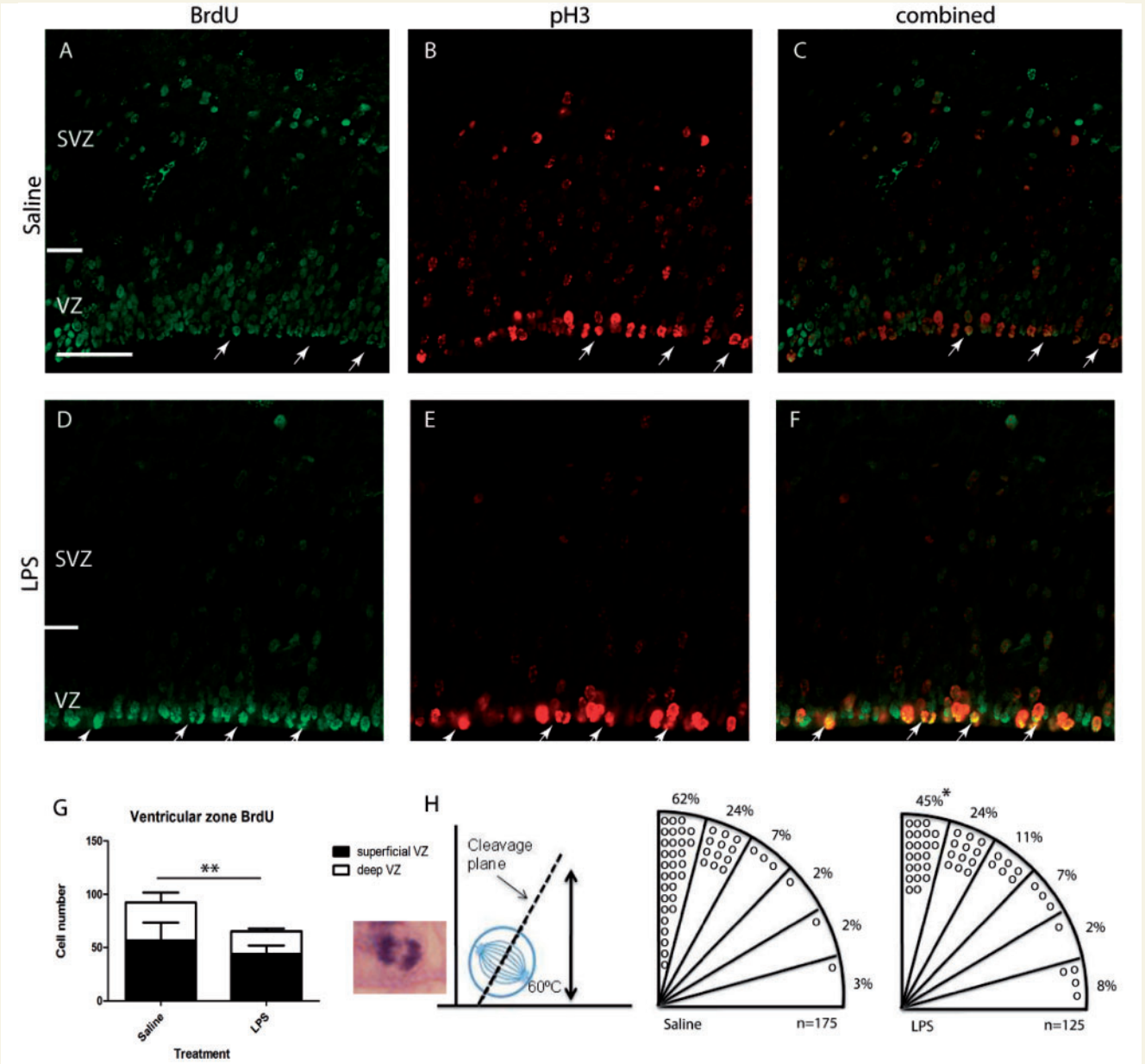

Figure 2 Comparison of bromodeoxyuridine (BrdU) uptake, pH3 immunoreactivity and mitotic cleavage phase between saline- and lipopolysaccharide- (10 μg/kg) treated animals in embryonic Day 13.5 mice at 8 h post injection. In control animals, bromodeoxyuridine-labelled cells (green, **A**, **C**) were found in the ventricular zone (VZ) and subventricular zone (SVZ). A number of the bromodeoxyuridine-positive cells co-labelled with pH3 at the ventricular surface (red, **B**, **C**). In lipopolysaccharide-treated animals, fewer bromodeoxyuridine- and pH3-positive cells were observed compared with controls, but a higher proportion of pH3-positive cells co-labelled with bromodeoxyuridine (**D–G**), arrows indicate double-labelled cells. (**H**) Angle of mitotic (anaphase) cleavage was assessed from haematoxylin and eosin-stained sections as shown. There was a significant decrease in the number of cells with a cleavage plane between 75° and 90° in lipopolysaccharide-treated animals compared with controls, with a proportional increase in numbers of cells with an angle $<60°$. Scale bar = 50 μm. $^{**}P < 0.005$. LPS = lipopolysaccharide.

the choroid plexus and taken up into these cells, plasma proteins are not normally detected in the brain parenchyma by immunohistochemistry. Presence of these proteins in the brain typically reflects altered blood–brain or blood–CSF barrier permeability (Stolp *et al*., 2005). In foetal brains from saline-injected animals (embryonic Day 14), plasma protein immunoreactivity was observed within the CSF, in the meninges at the surface of the brain, and the cerebral blood vessels (Fig. 4A). In the brains of embryonic Day 13.5 foetuses from lipopolysaccharide-treated dams 8 h after injection, plasma protein immunoreactivity was similarly observed in all of these locations, but was also found within some cells at the ventricular surface (Fig. 4B–D). While only a small number of plasma protein-positive cells (an average of 14 ± 5 per section) were observed in brains from 10 μg/kg

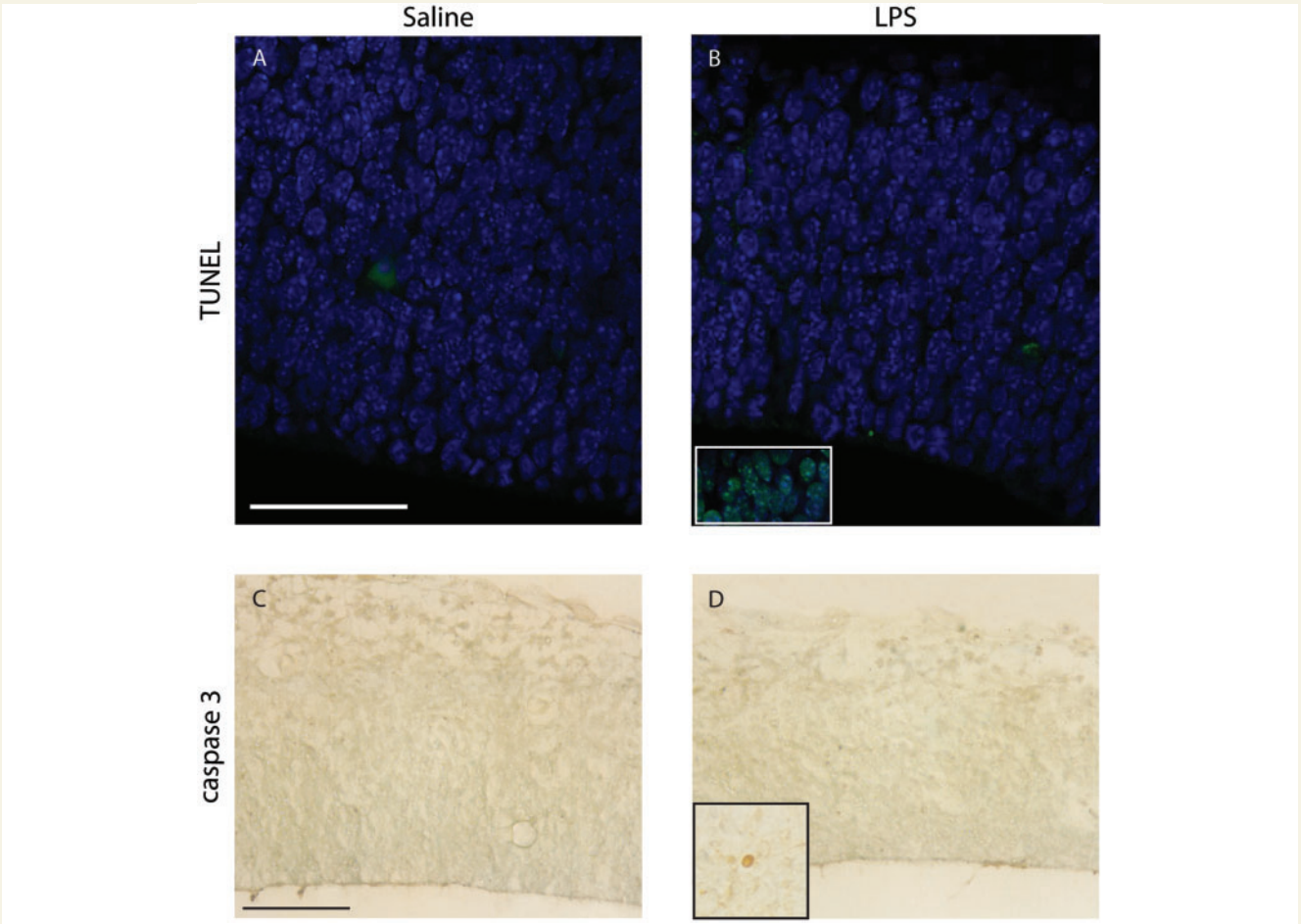

Figure 3 No TUNEL or active caspase 3-positive cells were observed in either saline- or lipopolysaccharide-treated brains at embryonic Day 14. In TUNEL-stained tissue, only non-specific fluorescence of red blood cells within the blood vessels can be seen (**A**, **B**), compared with the DNaseI-treated positive control (insert in **B**). In active caspase 3-stained tissue, no immunoreactivity can be observed (**C**, **D**). Insert in **D** indicates active caspase 3-positive cells in control post-natal Day 8 tissue, indicating normal developmental cell death. Scale bar = 50 μm.

lipopolysaccharide-treated animals; this was significantly greater than the number of plasma protein-positive cells identified on the ventricular surface in control brains (1 ± 1 per section, $P = 0.04$). In the high-dose lipopolysaccharide treatment (500 μg/kg) at embryonic Day 14, the number of plasma protein-positive cells within the ventricular zone was even higher (compare Fig. 4B and C). Cells that were positive for plasma proteins were confirmed to be radial progenitor cells by co-localization with acetylated tubulin (Fig. 4D–F). There was disruption in the organization of the radial progenitors at the ventricular surface, particularly their projections towards the pial surface. This varied in degrees between animals (compare Fig. 4H1 and H2) and appeared to be dose dependent, as changes were most prominent in the high-dose lipopolysaccharide-treated animals (Fig. 4I).

Adherens and tight junctions

In saline-treated foetuses at embryonic Day 14 (8 h after injection), β-catenin immunoreactivity can be observed along the entire ventricular surface in a clear and well-defined band (Fig. 5A), which reflects the presence of adherence junctions at the boundary between the brain parenchyma and the CSF. Similar to the radial progenitor's acetylated tubulin staining (Fig. 4), a range of staining patterns was observed within both the low- and high-dose lipopolysaccharide-treated animals. In some cases, normal staining of the ventricular surface was present, which was occasionally combined with stained debris in the CSF near the ventricular surface (Fig. 5B and D). Alternatively, a patchy presence of the protein along the ventricular surface could be seen, particularly in the high-dose lipopolysaccharide-treated animals (Fig. 5C and D). In these animals, cellular debris within the CSF, associated with the ventricular surface, which partially stained for β-catenin, was identified.

In contrast to the staining of the ventricular surface, between saline- and lipopolysaccharide-treated animals there was no alteration in β-catenin immunoreactivity in blood vessels in this region (Fig. 5E and F), nor was there an alteration in the tight junction proteins occludin (Fig. 5G and H) and claudin-5 (Fig. 5I and J).

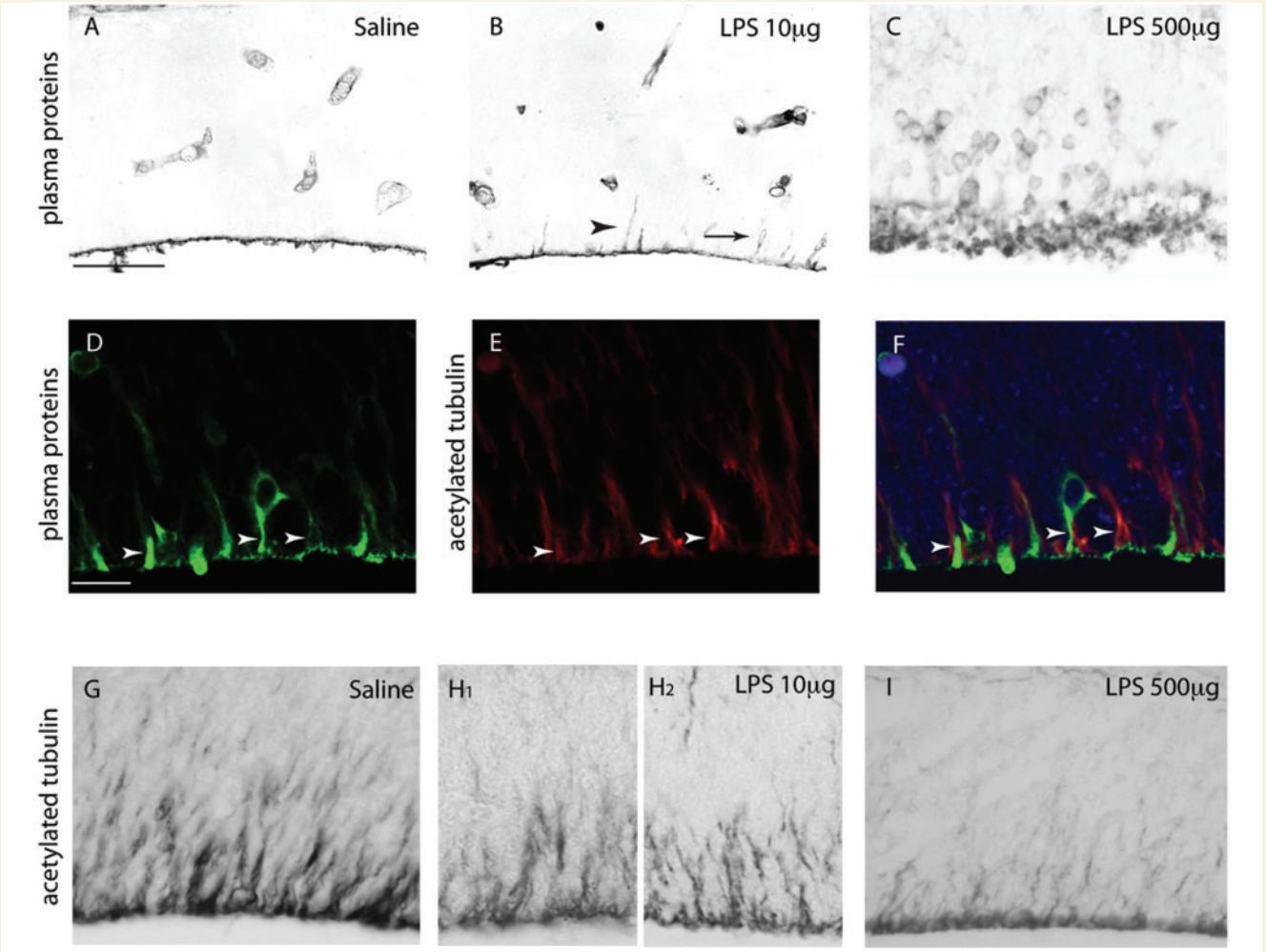

Figure 4 Comparison of plasma protein uptake by radial progenitor cells at the ventricular surface in saline- and lipopolysaccharide-treated tissue at embryonic Day 14. Plasma protein immunoreactivity was only observed in the blood vessels, CSF and meninges in brains from saline-exposed foetuses (**A**). In foetal brains from dams exposed to lipopolysaccharide (LPS, 10 μg/kg), there was no change in the permeability of the blood–brain barrier in vessels in the cortex to the plasma protein, but protein-positive cells were observed at the ventricular surface; these were much more frequent in the higher dose lipopolysaccharide animals (**B**, **C**). The plasma protein immunoreactivity co-localized with acetylated tubulin (**D–F**), which stains the radial progenitor cells in the ventricular zone. Acetylated tubulin-positive radial progenitor cells were reduced in number in lipopolysaccharide-treated animals compared with controls, an effect that was variable between litters (H1 compared with H2) much greater at the higher dose (**G–I**). Scale bar: **A–C**, **G–I** = 50 μm; **D–F** = 10 μm. Arrow heads in **B** indicate plasma protein positive cells. Arrow heads in Figure **D–F** represent double labelled cells.

No occludin or claudin-5 immunoreactivity was detected at the ventricular surface in either group.

Cortical response at embryonic Day 15.5

In the cortex of foetal animals at embryonic Day 15.5, treated with lipopolysaccharide at embryonic Day 13.5, there was a residual presence of plasma proteins within the cells both within the ventricular zone (Fig. 6B) and the developing cortical plate (Fig. 6C) compared with saline-treated animals (Fig. 6A). However, there were no gross changes in acetylated-tubulin-stained radial glia 48 h following lipopolysaccharide compared with saline injected controls, or in β-catenin immunoreactivity at the ventricular surface (data not shown). Cells undergoing mitosis, identified by pH3 immunoreactivity, were not significantly different in number between controls and animals exposed to inflammation (Fig. 6D). The entire ventricular zone and subventricular zone proliferative regions were also assessed with Pax6 and Tbr2 immunoreactivity, respectively. There was no significant difference in the proportion or the position of the cortex that expressed Pax6 or Tbr2 indicating the ventricular and subventricular proliferative regions within the cortex at embryonic Day 15.5 (Fig. 6E–I).

Cortical layering at post-natal Day 8

Adult-like cortical laminar structure, with completed cortical migration and expression of layer-specific markers, is established from approximately post-natal Day 8 in the mouse brain. The cortical

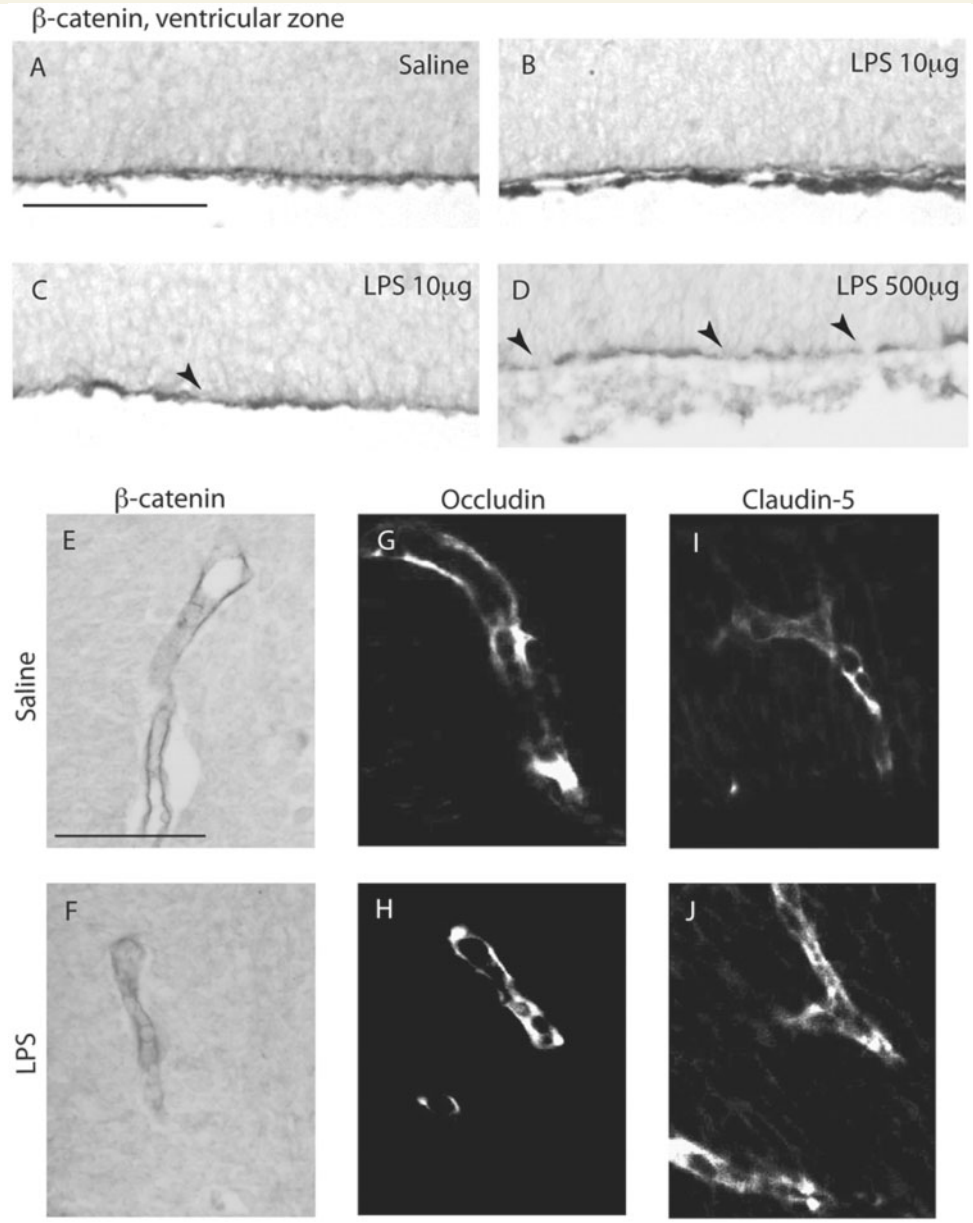

Figure 5 Comparison of junctional integrity at the ventricular surface and in the cerebral microvasculature in saline- and lipopolysaccharide-treated tissue. β-catenin is a major constituent of the adherence junctions between the cells at the ventricular surface. (**A**) β-catenin immunoreactivity along the ventricular surface of an embryonic Day 14 foetus from saline-treated animals. (**B–D**) Embryonic Day 14 foetuses from low (**B**, **C**) and high (**D**) lipopolysaccharide (LPS) dose-treated animals showed a variety of β-catenin immunoreactivity, including disturbed immunoreactivity along the ventricular surface (arrowheads, **C**, **D**). β-catenin immunoreactivity of the adherens junctions in the blood vessels was not altered with treatment (**E**, **F**), nor was the immunoreactivity of the tight junction proteins occludin and claudin-5 (**G–I**). Scale bars = 50 μm.

cytoarchitecture was assessed using the pan-neuronal marker NeuN and demonstrated clear cortical layering (Fig. 7A and D). The majority of neurons destined for Layer V, and to some extent Layer IV, are born between embryonic Days 13 and 14.5 (Molyneaux *et al*., 2007). This is the period when decreased proliferation was observed following maternal inflammation (Fig. 1). We directed our examination specifically to these populations to study whether there was a longer term alteration at these later stages of development. We therefore stained with antibodies against specific neuronal markers for these layers; CTIP2 for Layer V and ROR for Layer IV. Statistically significant increases in density of labelled cells were found within both Layers V and IV following systemic maternal inflammation compared with saline-treated groups. Layer V neurons went from a density of 300 ± 26 cells/mm^2 in control tissue to 402 ± 6 cells/mm^2 following maternal lipopolysaccharide treatment, an increase of 33% ($P = 0.007$). Layer IV had a higher number of cells per area compared with Layer V, with 1930 ± 117 cells/mm^2 in control

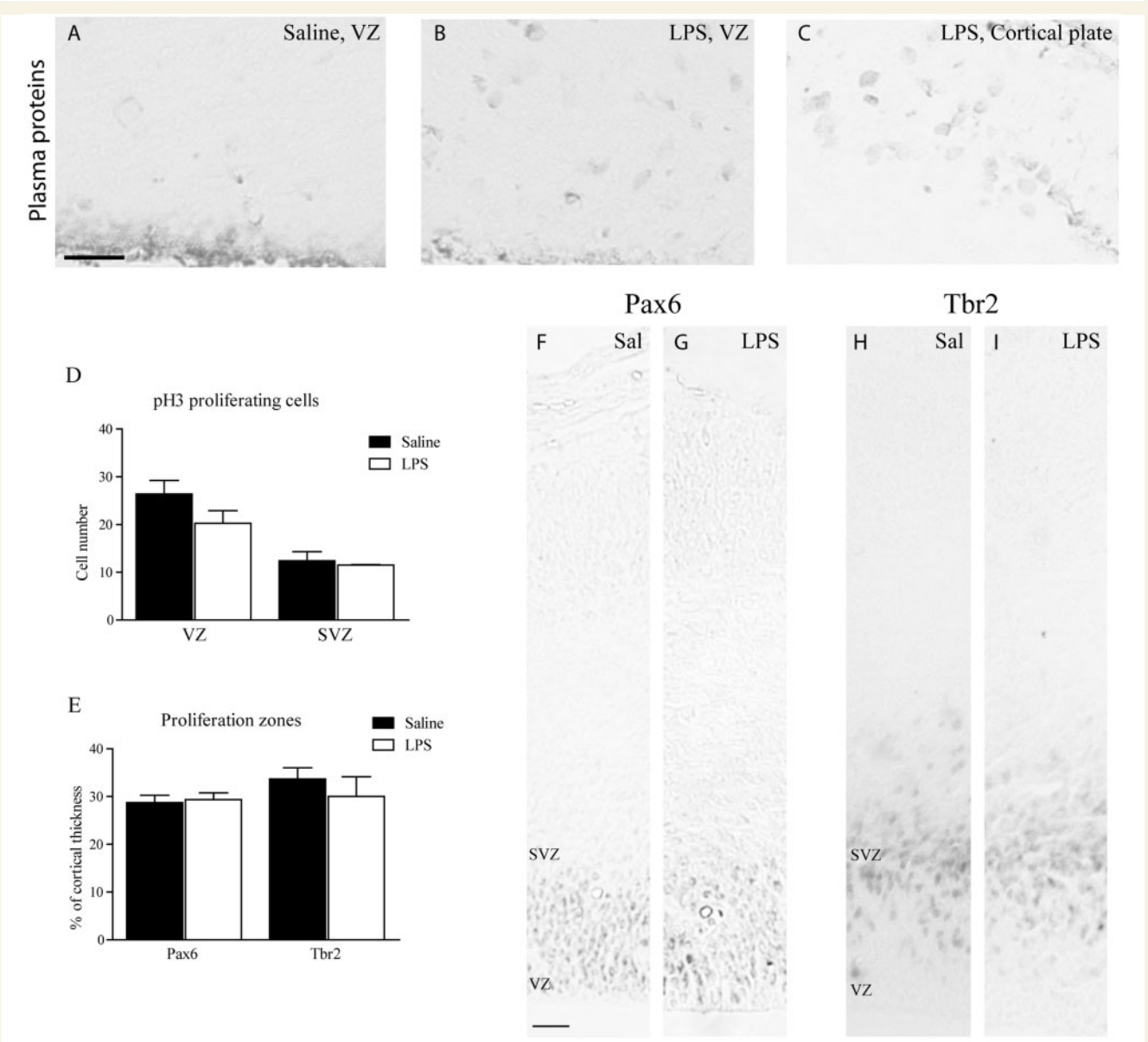

Figure 6 Consequences of maternal inflammation induced at embryonic Day 13.5 on the cortical plate and ventricular zone and subventricular zone proliferative zones at embryonic Day 15.5. Plasma protein immunoreactivity was found in cells of the ventricular zone (VZ) and cortical plate 48 h following maternal inflammation (**B**, **C**) but was only visible along the ventricular surface in saline-treated animals at embryonic Day 15 (**A**). No difference was observed in the number of mitotic cells (**D**) or proportions of the ventricular proliferative zone (**E**) represented by Pax6 immunoreactivity (**F**, **G**) and the Tbr2 immunoreactive subventricular zone (SVZ, **H**, **I**) at embryonic Day 15.5 following maternal lipopolysaccharide treatment compared with saline- (sal) treated controls. Scale bar = 25 μm.

animals. This increased by 40% to 2728 ± 39 cells/mm^2 in lipopolysaccharide-treated animals ($P = 0.003$, Fig. 6G).

Discussion

Maternal inflammation during foetal development has been linked to a wide variety of long-term behavioural changes associated with human neurodevelopmental disorders (Nelson and Grether, 1999; Pardo and Eberhart, 2007; O'Shea *et al.*, 2009; Brown, 2011). The present study shows, for the first time, the immediate effect of maternal inflammation on the developing brain and may provide some clues towards the understanding of the molecular and cellular mechanisms of developmentally acquired neurological disorders. It also demonstrates that these changes lead to prolonged alterations of the cortical cytoarchitecture during post-natal life.

Neurogenesis

The results of this study clearly show a short-term decrease in proliferation in the ventricular zone of the developing neocortex, that occurred within 8 h of onset of maternal inflammation (Fig. 1)

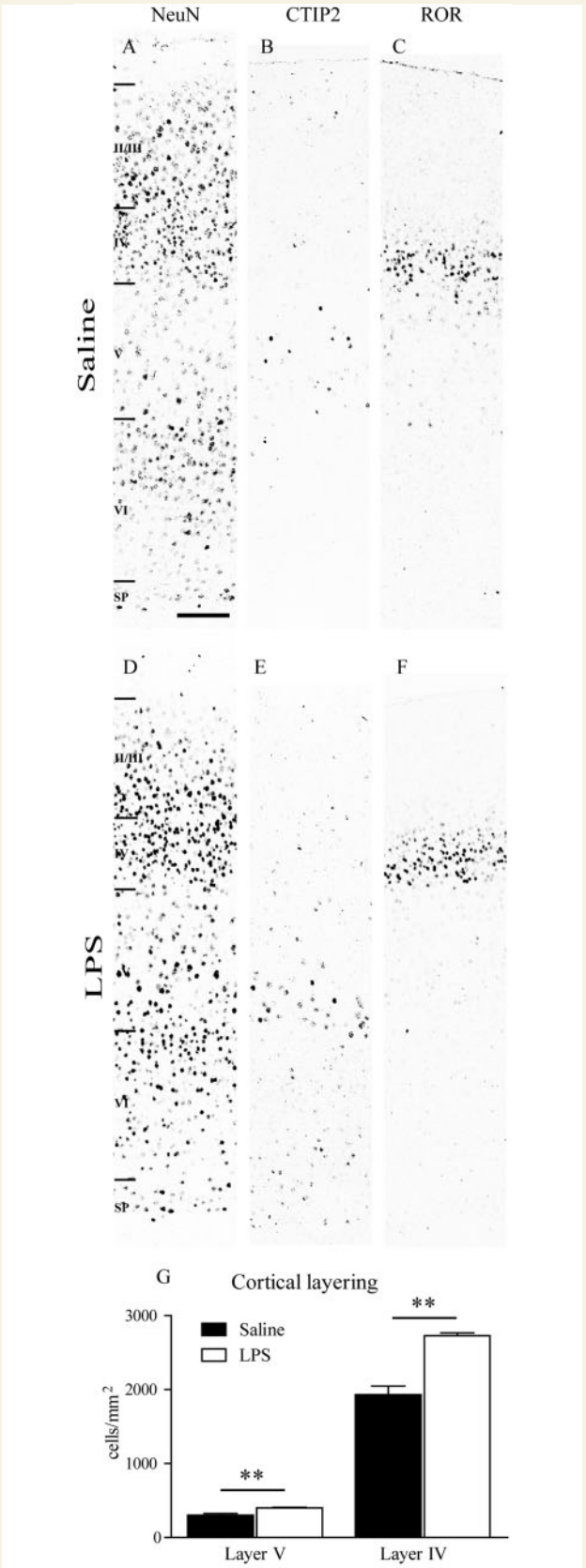

Figure 7 Prolonged effect of maternal inflammation on cortical layering at post-natal Day 8. Animals exposed to saline or lipopolysaccharide (LPS, 10 μg/kg) at embryonic Day 13.5 of pregnancy were examined at post-natal Day 8. There was no gross change in cortical layering or thickness based on NeuN staining (**A**, **D**). An increased density of cells within Layers V (**B**, **E**) and IV (**C**, **F**), but not the position of the layers, was observed based on CTIP2 and ROR staining, respectively. Scale bar: **A–E** = 100 μm. $^{**}P < 0.01$. SP = subplate.

and has returned to control levels by the time inflammation had resolved, 48 h following maternal lipopolysaccharide injection (Fig. 6D). At embryonic Day 13.5 in the mouse, the ventricular zone typically divides either symmetrically, to produce radial progenitor cells that increase the size of the proliferative pool, or to a lesser degree, asymmetrically producing either neurons that populate the cortical plate, typically Layer V (Angevine and Sidman, 1961; Molyneaux *et al.*, 2007) or a secondary progenitor pool in the subventricular zone (Haubensak *et al.*, 2004; Miyata *et al.*, 2004; Noctor *et al.*, 2004). The type of division undertaken appears to be regulated by the length of the cell cycle, particularly the length of G1 and the switch to S1 (Dehay and Kennedy, 2007) regulated by cyclin E1 (Moroy and Geisen, 2004). The angle of mitosis (vertical or horizontal during M phase) is also an indicator of the differentiation process (Dehay and Kennedy, 2007). The reduction in bromodeoxyuridine labelling observed in the present study (Fig. 2) indicates that, within 2 h of the maternal inflammatory response, a decreased number of cells are entering S phase, an observation that is supported by the trend towards reduced cyclin E1 expression at 8 h. The shift in the mitotic angle away from vertical (Fig. 2H), along with the apparent lengthening of the G1 phase of division, suggests that along with a general reduction in proliferation, there is relatively more asymmetric division occurring in those cells still entering the cell cycle. This hypothesis is supported by the increased density of cells in Layers V and IV observed at post-natal Day 8. No change was seen in the size of the proliferating zones at embryonic Day 15 or in the density of the other cortical layers at post-natal Day 8, implying that despite the shift towards asymmetric division there is no long-term reduction in the proliferative pool. The shortening of the radial progenitor projections, shown by altered acetylated tubulin immunoreactivity (Fig. 4), suggests that a migration deficit may accompany the reduced proliferation following this insult (Creppe *et al.*, 2009); however, plasma protein-positive cells appeared to migrate from the ventricular zone to the cortical plate between embryonic Days 13.5 and Day 15 (Fig. 6C) and no tangible changes in layering were observed in the cortex at post-natal Day 8.

Nevertheless, it is a possibility that the increase in cell density in Layers V and IV at post-natal Day 8 (Fig. 7), notwithstanding the reduction in ventricular zone proliferation at embryonic Day 14, indicates that the latter decrease is followed by a phase of overcompensation. Given that lipopolysaccharide was only administered as a single dose, it may be that evoking a more prolonged maternal inflammatory response might result in a permanent deficit in ventricular zone proliferation and consequently a subsequent reduction in cell numbers in Layers V and IV. A practical consequence of the present findings could be that early intervention to treat maternal infection might ameliorate a potentially detrimental

effect on the proliferating ventricular zone and subsequent brain development, should it remain untreated. The long-term development of these cortical layers and their interactions and integration throughout the brain, following brief or prolonged maternal inflammation will require further study to fully elucidate the consequences of these changes in maternal inflammation during pregnancy. Such studies will have to be coupled with lineage analysis of cortical neurons.

Ventricular integrity

Proliferation at the ventricular surface appears to be partially regulated by the nature of the adherens junctions at the apical end-feet of the radial progenitor cells (Sottocornola *et al.*, 2010). It has been shown in foetuses during the period of neurogenesis that there are membrane specializations between adjacent cells ('strap' junctions) that prevent the passage of protein from CSF to the interstitial space of the brain parenchyma (Fossan *et al.*, 1985; Møllgård *et al.*, 1987). β-catenin, associated with N-cadherin, is a key molecule in the association between ependymal adherens junctions and ventricular proliferation (Junghans *et al.*, 2005). Loss of β-catenin from the anterolateral telencephalon from E10 has been associated with the loss of adherens junctions and structural integrity of the ventricular surface (Junghans *et al.*, 2005). In these FoxG1-β-catenin mutant mice, cellular debris that was derived from the damaged ventricular surface was identified in the CSF, a similar observation to that of the present study in animals exposed to the high dose of lipopolysaccharide (Fig. 5). While no change in proliferation was associated with the FoxG1-β-catenin mutation (Junghans *et al.*, 2005), β-catenin has been associated with the regulation of cell division through the canonical Wnt signalling pathway (Zhou *et al.*, 2006; Kuwahara *et al.*, 2010), highlighting β-catenin as key in the inflammation-induced altered ventricular zone proliferation observed in the present study. The altered junctions at the ventricular surface may also contribute to the reduced proliferation observed, by allowing the penetration of plasma proteins into the brain, and thereby the radial progenitor cells, from the CSF (proteins that are specifically transported into the CSF during development; see Liddelow *et al.*, 2009). Plasma proteins have been identified as cytotoxic when introduced to the adult brain (Nordborg *et al.*, 1991; Wagner *et al.*, 2002), although in the present study no evidence of cell death was found during the time frame examined (Fig. 3) and plasma protein-positive cells were still present within the cortex at embryonic Day 15, 48 h after induction of the inflammatory response. However, it is interesting to note that in the subventricular zone, where the vascular plexus maintained its tight junctions and integrity (Figs 4B and 5G–J), there was less of an effect on cell proliferation than in the ventricular zone, suggesting that the presence of the plasma proteins in the ventricular zone could be contributing to the decreased proliferation.

Physiological mechanism

The mechanism by which maternal inflammation can affect foetal brain development remains unclear, as it has been shown that lipopolysaccharide does not cross the placental barrier (Ashdown *et al.*, 2006). Inflammation during late gestation causes reduced placental perfusion (Girard *et al.*, 2010), suggesting that hypoxia–ischaemia may contribute to the foetal pathology. An increased expression of inflammatory mediators has been observed in the placenta (Girard *et al.*, 2010) and the foetal brain (Meyer *et al.*, 2006). In the present study, despite the comparatively low dose of lipopolysaccharide used (10 μg/kg) a maternal and placental inflammatory response was detected (Stolp *et al*., unpublished data). The foetal immune response and subsequent injury vary with gestational age and suggest that the maturation of the foetal immune response may also contribute to the variety and magnitude of neuropathologies observed in the developing brain following maternal inflammation. The brain region injured by insult at different stages of disease may be partly based on the developmental timetable of the specific structure as well as the maturity and intensity of the foetal immune response. This hypothesis is supported by the work of Fortier *et al*. (2007) showing that prepulse inhibition following maternal inflammation varies both with foetal age and inflammatory mediator. It is important to consider this possibility in the light of other neurodevelopmental disorders.

Conclusion

The results of the present study show that maternal inflammation has not only an immediate consequence for the development of the foetal cortex, but also a long-term effect on cortical cytoarchitecture and structure during post-natal life. However, whether these alterations are compensated for or the cell numbers and cells types are altered permanently is currently unknown. The decreased proliferation, resulting from a reduction in the adherens junctions at the ventricular surface, and a change in differentiation following proliferation, may affect several aspects of cortical growth and connection with subcortical areas. Yet to be determined is the relative effect of inflammation on other brain areas, changes in the hippocampus and cerebellum have also been reported, as well as the cortex (Fatemi *et al.*, 2002, 2008*b*; Golan *et al.*, 2005; Meyer *et al.*, 2006, 2008). It will be interesting to see in future studies how the interactions between these areas of damage contribute to the altered neurological behaviour observed.

The nature of inflammation-induced neural damage is likely to be dependent both on the stage of cortical development and the stage of development of the foetal immune system at the time of the insult. In addition, this study suggests that maternal inflammation can result in long-term behavioural changes by disrupting cortical development and suggests that the current therapy for clinical management of maternal inflammation should be further evaluated.

Acknowledgements

Our thanks go to Dr Sandra Campbell, Dr Francis Szele, Dr Isabelle Comte, Dr Anna Hoerder-Suabeddissen and Dr Zoltan Sarnyai for their thoughtful comments and discussions.

Funding

St John's College Research Centre, Oxford; European Union (HEALTH-F2-2009-241778) Neurobid Consortium, funded by the Seventh Framework Program and NHMRC; National Health and Medical Research Council, Australia (grant #454399); Medical Research Council, United Kingdom (grant #G0700377, #G00900901).

References

Angevine JB Jr, Sidman RL. Autoradiographic study of cell migration during histogenesis of cerebral cortex in the mouse. Nature 1961; 192: 766–8.

Ashdown H, Dumont Y, Ng M, Poole S, Boksa P, Luheshi GN. The role of cytokines in mediating effects of prenatal infection on the fetus: implications for schizophrenia. Mol Psychiatry 2006; 11: 47–55.

Brown AS. The environment and susceptibility to schizophrenia. Prog Neurobiol 2011; 93: 23–58.

Cheung AF, Kondo S, Abdel-Mannan O, Chodroff RA, Sirey TM, Bluy LE, et al. The subventricular zone is the developmental milestone of a 6-layered neocortex: comparisons in metatherian and eutherian mammals. Cereb Cortex 2010; 20: 1071–81.

Clancy B, Darlington RB, Finlay BL. Translating developmental time across mammalian species. Neuroscience 2001; 105: 7–17.

Clancy B, Finlay BL, Darlington RB, Anand KJS. Extrapolating brain development from experimental species to humans. NeuroToxicology 2007; 28: 931–7.

Creppe C, Malinouskaya L, Volvert ML, Gillard M, Close P, Malaise O, et al. Elongator controls the migration and differentiation of cortical neurons through acetylation of alpha-tubulin. Cell 2009; 136: 551–64.

Dehay C, Kennedy H. Cell-cycle control and cortical development. Nat Rev Neurosci 2007; 8: 438–50.

Dziegielewska KM, Evans CAN, Malinowska DH, Møllgård K, Reynolds ML, Saunders NR. Blood-cerebrospinal fluid transfer of plasma proteins during fetal development in the sheep. J Physiol 1980; 300: 457–65.

Dziegielewska KM, Møllgård K, Saunders NR, Reader M. Fetuin synthesis in cells of the immature neocortex. J Neurocytol 1993; 22: 266–72.

Dziegielewska KM, Daikuhara Y, Ohnishi T, Waite PME, Ek J, Habgood MD, et al. Fetuin in the developing neocortex of the rat: distribution and origin. J Comp Neurol 2000; 423: 373–88.

Fatemi SH, Earle J, Kanodia R, Kist D, Emamian ES, Patterson PH, et al. Prenatal viral infection leads to pyramidal cell atrophy and macrocephaly in adulthood: implications for genesis of autism and schizophrenia. Cell Mol Neurobiol 2002; 22: 25–33.

Fatemi SH, Reutiman TJ, Folsom TD, Huang H, Oishi K, Mori S, et al. Maternal infection leads to abnormal gene regulation and brain atrophy in mouse offspring: implications for genesis of neurodevelopmental disorders. Schizophr Res 2008a; 99: 56–70.

Fatemi SH, Reutiman TJ, Folsom TD, Sidwell RW. The role of cerebellar genes in pathology of autism and schizophrenia. Cerebellum 2008b; 7: 279–94.

Fortier ME, Luheshi GN, Boksa P. Effects of prenatal infection on prepulse inhibition in the rat depend on the nature of the infectious agent and the stage of pregnancy. Behav Brain Res 2007; 181: 270–7.

Fossan G, Cavanagh ME, Evans CA, Malinowska DH, Møllgård K, Reynolds ML, et al. CSF-brain permeability in the immature sheep fetus: a CSF-brain barrier. Brain Res 1985; 350: 113–24.

Girard S, Kadhim H, Beaudet N, Sarret P, Sebire G. Developmental motor deficits induced by combined fetal exposure to lipopolysaccharide and early neonatal hypoxia/ischemia: a novel animal model for cerebral palsy in very premature infants. Neuroscience 2009; 158: 673–82.

Girard S, Tremblay L, Lepage M, Sebire G. IL-1 receptor antagonist protects against placental and neurodevelopmental defects induced by maternal inflammation. J Immunol 2010; 184: 3997–4005.

Golan HM, Lev V, Hallak M, Sorokin Y, Huleihel M. Specific neurodevelopmental damage in mice offspring following maternal inflammation during pregnancy. Neuropharmacology 2005; 48: 903–17.

Habgood MD, Sedgwick JEC, Dziegielewska KM, Saunders NR. A developmentally regulated blood-cerebrospinal fluid transfer mechanism for albumin in immature rats. J Physiol 1992; 456: 181–92.

Haubensak W, Attardo A, Denk W, Huttner WB. Neurons arise in the basal neuroepithelium of the early mammalian telencephalon: a major site of neurogenesis. Proc Natl Acad Sci USA 2004; 101: 3196–201.

Hava G, Vered L, Yael M, Mordechai H, Mahoud H. Alterations in behavior in adult offspring mice following maternal inflammation during pregnancy. Dev Psychobiol 2006; 48: 162–8.

Junghans D, Hack I, Frotscher M, Taylor V, Kemler R. Beta-catenin-mediated cell-adhesion is vital for embryonic forebrain development. Dev Dyn 2005; 233: 528–39.

Kuwahara A, Hirabayashi Y, Knoepfler PS, Taketo MM, Sakai J, Kodama T, et al. Wnt signaling and its downstream target N-myc regulate basal progenitors in the developing neocortex. Development 2010; 137: 1035–44.

Liddelow SA, Dziegielewska KM, Ek CJ, Johansson PA, Potter AM, Saunders NR. Cellular transfer of macromolecules across the developing choroid plexus of Monodelphis domestica. Eur J Neurosci 2009; 29: 253–66.

Liddelow SA, Dziegielewska KM, Vandeberg JL, Noor NM, Potter AM, Saunders NR. Modification of protein transfer across blood/cerebrospinal fluid barrier in response to altered plasma protein composition during development. Eur J Neurosci 2011; 33: 391–400.

Meyer U, Feldon J, Schedlowski M, Yee BK. Towards an immunoprecipitated neurodevelopmental animal model of schizophrenia. Neurosci Biobehav Rev 2005; 29: 913–47.

Meyer U, Nyffeler M, Engler A, Urwyler A, Schedlowski M, Knuesel I, et al. The time of prenatal immune challenge determines the specificity of inflammation-mediated brain and behavioral pathology. J Neurosci 2006; 26: 4752–62.

Meyer U, Nyffeler M, Yee BK, Knuesel I, Feldon J. Adult brain and behavioral pathological markers of prenatal immune challenge during early/middle and late fetal development in mice. Brain Behav Immun 2008; 22: 469–86.

Miyata T, Kawaguchi A, Saito K, Kawano M, Muto T, Ogawa M. Asymmetric production of surface-dividing and non-surface-dividing cortical progenitor cells. Development 2004; 131: 3133–45.

Møllgård K, Balslev Y, Lauritzen B, Saunders NR. Cell junctions and membrane specializations in the ventricular zone (germinal matrix) of the developing sheep brain: a CSF-brain barrier. J Neurocytol 1987; 16: 433–44.

Molyneaux BJ, Arlotta P, Menezes JR, Macklis JD. Neuronal subtype specification in the cerebral cortex. Nat Rev Neurosci 2007; 8: 427–37.

Moroy T, Geisen C. Cyclin E. Int J Biochem Cell Biol 2004; 36: 1424–39.

Nawa H, Takei N. Recent progress in animal modeling of immune inflammatory processes in schizophrenia: implication of specific cytokines. Neurosci Res 2006; 56: 2–13.

Nelson KB, Grether JK. Causes of cerebral palsy. Curr Opin Pediatr 1999; 11: 487–91.

Noctor SC, Martinez-Cerdeno V, Ivic L, Kriegstein AR. Cortical neurons arise in symmetric and asymmetric division zones and migrate through specific phases. Nat Neurosci 2004; 7: 136–44.

Nordborg C, Sokrab TE, Johansson BB. The relationship between plasma protein extravasation and remote tissue changes after experimental brain infarction. Acta Neuropathol 1991; 82: 118–26.

Nyffeler M, Meyer U, Yee BK, Feldon J, Knuesel I. Maternal immune activation during pregnancy increases limbic GABAA receptor immunoreactivity in the adult offspring: implications for schizophrenia. Neuroscience 2006; 143: 51–62.

O'Shea TM, Allred EN, Dammann O, Hirtz D, Kuban KC, Paneth N, et al. The ELGAN study of the brain and related disorders in extremely low gestational age newborns. Early Hum Dev 2009; 85: 719–25.

Pardo CA, Eberhart CG. The neurobiology of autism. Brain Pathol 2007; 17: 434–47.

Pramparo T, Youn YH, Yingling J, Hirotsune S, Wynshaw-Boris A. Novel embryonic neuronal migration and proliferation defects in Dcx mutant mice are exacerbated by Lis1 reduction. J Neurosci 2010; 30: 3002–12.

Rakic P, Caviness VS Jr. Cortical development: view from neurological mutants two decades later. Neuron 1995; 14: 1101–4.

Rice D, Barone S. Critical periods of vulnerability for the developing nervous system: evidence from humans and animal models. Environ Health Perspect 2000; 108 (Suppl. 3): 511–33.

Rehn AE, Rees SM. Investigating the neurodevelopmental hypothesis of schizophrenia. Clin Exp Pharmacol Physiol 2005; 32: 687–96.

Shi L, Fatemi SH, Sidwell RW, Patterson PH. Maternal influenza infection causes marked behavioral and pharmacological changes in the offspring. J Neurosci 2003; 23: 297–302.

Sottocornola R, Royer C, Vives V, Tordella L, Zhong S, Wang Y, et al. ASPP2 binds Par-3 and controls the polarity and proliferation of neural progenitors during CNS development. Dev Cell 2010; 19: 126–37.

Stolp HB, Dziegielewska KM, Ek CJ, Habgood MD, Lane MA, Potter AM, et al. Breakdown of the blood-brain barrier to proteins in white matter of the developing brain following systemic inflammation. Cell Tissue Res 2005; 320: 369–78.

Stolp HB, Johansson PA, Habgood MD, Dziegielewska KM, Saunders NR, Ek CJ. Effects of neonatal systemic inflammation on blood-brain barrier permeability and behaviour in juvenile and adult rats. Cardiovasc Psychiat Neurol 2011. Advance Access published on March 10, 2011, doi: 10.1155/2011/469046.

Wagner KR, Packard BA, Hall CL, Smulian AG, Linke MJ, De Courten-Myers GM, et al. Protein oxidation and heme oxygenase-1 induction in porcine white matter following intracerebral infusions of whole blood or plasma. Dev Neurosci 2002; 24: 154–60.

Wynshaw-Boris A, Pramparo T, Youn YH, Hirotsune S. Lissencephaly: mechanistic insights from animal models and potential therapeutic strategies. Semin Cell Dev Biol 2010; 21: 823–30.

Zhou CJ, Borello U, Rubenstein JL, Pleasure SJ. Neuronal production and precursor proliferation defects in the neocortex of mice with loss of function in the canonical Wnt signaling pathway. Neuroscience 2006; 142: 1119–31.